



PII S0016-7037(01)00877-8

Unraveling the atomic structure of biogenic silica: Evidence of the structural association of Al and Si in diatom frustules

M. GEHLEN,^{1,*} L. BECK,² G. CALAS,³ A. -M. FLANK,⁴ A. J. VAN BENNEKOM,⁵ and J. E. E. VAN BEUSEKOM⁶¹Laboratoire des Sciences du Climat et de l'Environnement (LSCE), Orme des Merisiers, Bât. 709, CEA/Saclay, 91191 Gif-sur-Yvette cedex, France²Laboratoire de Minéralogie-Cristallographie, Universités Paris 6 et 7 and IPG, 4 place Jussieu, 75252 Paris cedex, France³LEMFI/INSTN-DRECAM, CEA/Saclay, 91191 Gif-sur-Yvette cedex, France⁴LURE, CEA/CNRS/MEN, Bât. 209D, BP 34, 91898 Orsay cedex, France⁵NIOZ, P.O. Box 59, 1790 AB Den Burg, the Netherlands⁶AWI, Wattenmeerstation Sylt, Hafenstrasse 43, 25992 List/Sylt, Germany

(Received November 12, 2001; accepted November 12, 2001)

Abstract—We used X-ray absorption spectroscopy at the Al K-edge to investigate the atomic structure of biogenic silica and to assess the effect of Al on its crystal chemistry. Our study provides the first direct evidence for a structural association of Al and Si in biogenic silica. In samples of cultured diatoms, Al is present exclusively in fourfold coordination. The location and relative intensity of X-ray absorption near-edge structure (XANES) features suggests the structural insertion of tetrahedral Al inside the silica framework synthesized by the organism. In diatom samples collected in the marine environment, Al is present in mixed six- and fourfold coordination. The relative intensity of XANES structures indicates the coexistence of structural Al with a clay component, which most likely reflects sample contamination by adhering mineral particles. Extended X-ray absorption fine structure spectroscopy has been used to get Al-O distances in biogenic silica of cultured diatoms, confirming a tetrahedral coordination. Because of its effect on solubility and reaction kinetics of biogenic silica, the structural association between Al and biogenic silica at the stage of biosynthesis has consequences for the use of sedimentary biogenic silica as an indicator of past environmental conditions. Copyright © 2002 Elsevier Science Ltd

1. INTRODUCTION

Biogenic siliceous particles, made of amorphous, hydrated SiO₂, are produced in the upper water column as skeletal elements by diatoms, radiolaria, and silicoflagellates. Ocean waters are undersaturated (<100 μmol/L) with respect to biogenic Si, for which a solubility of 1000 μmol/L (2°C) has been reported (Tréguer et al., 1995). Despite its thermodynamic tendency to dissolve, a fraction of biogenic Si survives transfer through the water column and accumulates in abyssal sediments. Biogenic silica (BSi) is a major constituent of marine sediments, and its sedimentary record provides potentially valuable information of past ocean productivity and ecosystem structure. Our capability to interpret the sedimentary record of BSi in terms of past environmental conditions is presently limited by our lack of understanding of the processes controlling its preservation (Archer et al., 1993; McManus et al., 1995; Nelson et al., 1995).

The preservation of BSi is controlled by a competition between dissolution and removal from the undersaturated waters by burial. In surface sediments, the ongoing dissolution is revealed by the buildup of silicic acid (Si[OH]₄) in pore waters to quasi-constant levels below 5 to 30 cm deep. Reported asymptotic Si(OH)₄ levels range from 100 to 850 μmol/L (Hurd, 1973; Fanning and Pilson, 1974; Archer et al., 1993; McManus et al., 1995; Sayles et al., 1996; Rabouille et al., 1997) and are in general below the solubility of fresh plankton

assemblages (Lawson et al., 1978) or diatom cultures (Kamatani et al., 1980). Several hypotheses have been proposed to account for the lowered apparent solubility in sediments. Instead of reflecting a thermodynamic equilibrium between pore waters and the dissolving phase, asymptotic Si(OH)₄ might result from the kinetic competition between release of Si(OH)₄ from dissolving BSi and its uptake by the formation of aluminosilicate minerals (reverse weathering; Mackenzie and Garrels, 1966; Garrels and Mackenzie, 1971; Ristvet, 1978; Mackenzie et al., 1981). While Michalopoulos and Aller (1995) documented the importance of reverse weathering reactions for sediments of the Amazon river continental shelf, clay neof ormation driven by dissolved Al was verified experimentally by Dixit et al. (2001).

Alternatively, the solubility of BSi in marine sediments, after correction for pressure and temperature effects, might differ from estimates obtained for fresh plankton assemblages. Preferential dissolution of species with higher specific surface areas or fragile structures such as spines during the settling of diatom frustules through the water column results in a reduction of specific surface area of siliceous assemblages (Hurd et al., 1981; Hurd and Birdwhistell, 1983; Barker et al., 1994; Van Cappellen, 1996; Dixit et al., 2001). This process alone, however, cannot account for the apparent low solubilities of BSi in marine sediments (Dixit et al., 2001). After removal of the organic matrix, Al is the most important factor regulating the solubility of BSi (Lewin, 1961; Iler, 1973). The solubility is decreased significantly by only minor amounts of Al, >0.1% (Van Bennekom et al., 1989, 1991), compared to an average diatom Al/Si ratio of 1/1000 (Martin and Knauer, 1973). The

* Author to whom correspondence should be addressed (gehlen@lsce.saclay.cea.fr).

Table 1. Diatom samples discussed in this paper.

Species	Sample ID	Al (nmol/L) ^a	Si ($\mu\text{mol/L}$) ^a	Al/Si ^b	Ca/Si ^c	Ti/Si ^c
<i>Diatom cultures</i>						
<i>Porosira glacialis</i>	LV1	5	102	0.07×10^{-3}	$<1 \times 10^{-3}$	$<0.1 \times 10^{-3}$
<i>Thalassiosira nordenskjoeldii</i>	86	9	47	1.30×10^{-3}	2.2×10^{-3}	$<0.1 \times 10^{-3}$
<i>Thalassiosira nordenskjoeldii</i>	87	59	27	3.80×10^{-3}	3.5×10^{-3}	$<0.1 \times 10^{-3}$
<i>Lauderia annulata</i>	103	400	5	7.00×10^{-3}	5.4×10^{-3}	$<0.1 \times 10^{-3}$
<i>Natural diatom samples</i>						
Benthic assemblage	TF	Sample origin Wadden Sea tidal flat		8×10^{-3}	$<1 \times 10^{-3}$	0.4×10^{-3}
<i>Biddulphia sinensis</i>	BS	North Sea surface waters		8.30×10^{-3}	n.d.	n.d.

^a Dissolved Al and Si concentration in culture medium. For comparison, oceanic Al levels range from 20 to 200 nmol/L. High levels of 400 nmol/L were necessary during culture experiments to yield maximum Al/Si ratios. Note that the maximum elemental Al-to-Si ratio of cultured diatoms compares to natural samples.

^b Atomic Al/Si ratios determined by atomic absorption spectroscopy after complete digestion of frustules in HF/HCl/HNO₃ at 110°C or by particle-induced X-ray emission (PIXE) for sample TF.

^c Atomic Ca/Si ratios determined by PIXE after Beck et al. (in press). <0.1 stands for trace levels below the detection limit (PIXE); n.d., not determined.

interaction between BSi and dissolved Al produced by the dissolution of detrital minerals has been readdressed recently (Van Cappellen, 1996; Van Cappellen and Qiu, 1997a, 1997b; Dixit et al., 2001). The authors demonstrated the importance of diagenetic Al uptake by diatom frustules in modifying BSi solubility relative to that of fresh plankton assemblages.

The present study focuses on the association of Al with BSi. The underlying questions are, is Al incorporated into the frustules, or is it bound to the surface? If it is incorporated, can we identify a structural effect of its presence? While the structural incorporation of Al has been demonstrated for synthetic Si gels (Stone et al., 1993) and nonbiogenic low-temperature opals (Ildfonse and Calas, 1997), there is to date no conclusive evidence for the opal synthesized by diatoms. A straightforward analogy between synthetic gels, nonbiogenic mineral formation, and biomineralization might be misleading. We have used X-ray absorption spectroscopy (XAS) (Calas et al., 1984; Brown et al., 1988) to unravel the crystal chemistry of BSi and provide the first results on the structural association of Al with Si in diatom frustules. While Al K-edge X-ray absorption near-edge structure (XANES) spectra indicate the insertion of Al in the BSi framework of cultured diatoms in tetrahedral coordination, they reveal the coexistence of structural Al with smectite- and illite-type clay phases in natural marine diatom frustules. Extended X-ray fine structure (EXAFS) spectroscopy has been used to get Al-O distances in BSi of cultured diatoms, confirming a tetrahedral coordination.

2. MATERIAL

We compared diatom samples derived from cultures and the marine environment. Cultured diatoms were chosen to provide an end-member of known particle history on which the feasibility of our approach could be tested. Diatom samples used in this study are listed in Table 1 along with the corresponding atomic Al-to-Si ratios. Samples from diatom cultures *Porosira glacialis* (LV1) and *Thalassiosira nordenskjoeldii* (86) cover the low end of frustule Al-to-Si ratios. These ratios (Table 1) were too low for XAS.

Sample purity, the absence of adhering mineral particles, is of prime importance in the context of this study. We checked the mineralogy of natural diatoms by X-ray diffraction and,

within the detection limit of the analytical method, failed to detect contaminating mineral phases (e.g., clays). In a second approach, the bulk composition of cultured and natural diatoms was analyzed by particle-induced X-ray emission. The full data set is presented in Beck et al. (in press). In this paper, we present results (Table 1) for Ti as a tracer for a potential mineral contamination, along with Ca, the latter being relevant to the interpretation of XAS data. While Ti was below the detection limit in all cultured samples, significant levels were obtained for natural diatoms (Beck et al., in press). Titanium levels of the natural sample TF suggest the presence of mineral contaminants.

2.1. Diatom Cultures

Unialgal cultures of the marine diatoms *T. nordenskjoeldii* (Cleve; courtesy of Dr. Drebes, Biologische Anstalt Helgoland, List/Sylt, Germany), *Lauderia annulata* (courtesy of Dr. R. Riegman, Netherlands Institute for Sea Research, Texel, the Netherlands), and *P. glacialis* (courtesy of Dr. Admiraal, University of Groningen, the Netherlands) were used. The algae were kept in F/2 enriched seawater (Guillard and Ryther, 1962) at a temperature of 12°C under a 14/10 h light/dark cycle and dimmed light conditions ($\sim 100 \mu\text{Einstein/m}^2/\text{s}$).

For the experiments, batch cultures of both species were grown in artificial seawater (ASW). The ASW was prepared following the standard ocean seawater recipe (Morel et al., 1979), modified by adding a second cleaning step. Purification of ASW consisted of filtering the medium over an active coal filter to remove organic contaminants, followed by extraction of dissolved metals by an ion exchange resin (Chelex 100, 200- to 400- μm mesh) at pH 5. Final dissolved Al concentrations between 2 and 6 nmol/L were reached at a drip rate of approximately 120 cm³/h per column. A Si(OH)₄ stock solution was prepared by dissolving 1 g/dm³ silica gel in ASW at pH 8, yielding a final Si(OH)₄ concentration of 1400 $\mu\text{mol/dm}^3$. During the dissolution of the silica gel, no Al was set free (Van Beusekom, 1991). To avoid any contamination by heavy metals derived from the silica gel, the stock solution was purified by an ion exchange resin (Chelex 100) at pH 8. Nitrate and phosphate stocks were prepared from suprapure salts (Merck) and the

Table 2. Al-bearing references presented in this study.

Sample	CN	Origin	Composition	Al ^{IV} /Al ^{tot}	Ref.
Berlinite	4	Synthetic	AlPO ₄		1
Albite	4	Location unknown	NaAlSi ₃ O ₈		2
Kaolinite	6	Decazeville, France	Al ₂ Si ₂ O ₅ (OH) ₄		2
Muscovite	4, 6	LMCP	KAl ₂ (Si ₃ Al)O ₁₀ (OH) ₂	0.33	2
Smectite	4, 6	Prassa, Hungary	Na _{0.37} (Al _{1.58} Mg _{0.32} Ti _{0.01} Fe ³⁺ _{0.09}) (Si _{3.94} Al _{0.06})O ₁₀ (OH) ₂	0.03	2
Illite	4, 6	Puy en Velay, France	Na _{0.01} K _{0.64} Ca _{0.06} (Al _{1.19} Ti _{0.04} Fe ³⁺ _{0.36} Mn _{0.01} Mg _{0.43}) (Si _{3.53} Al _{0.47})O ₁₀ (OH) ₂	0.28	2
Opal-A	4	Salton Sea, USA	SiO ₂ Al/Si = 0.12		3

References: (1) Jumas et al. (1987), (2) Ildefonse et al. (1998), (3) Ildefonse and Calas (1997) CN = coordination number, LMCP = mineral collection of the Laboratoire de Minéralogie-Cristallographie, Paris).

vitamin stock from reagent-grade chemicals (Merck). The trace metal mix was prepared from a corresponding stock solution immediately before use. Aluminum was added separately from an Al stock solution based on reagent-grade AlCl₃. A NaHCO₃ solution was prepared immediately before use by dissolving 2 g of Na₂CO₃ (Baker, Ultrex) in 100 mL nanopure water and slowly adding 1.8 mL 30% HCl (Merck, suprapure). The enriched ASW was assembled by first slowly adding the NaHCO₃ solution. Care was taken to avoid carbonate precipitation. The pH was adjusted to 7.7 to 7.9, and vitamins, silicate, phosphate, nitrate, and trace metals were added. No EDTA was used to prevent complexation of Al. The seawater was filtered into acid-cleaned sterile 25-L polycarbonate culture vessels through cleaned 0.4- μ m membrane filters mounted on acid-cleaned filtration units. In Al-enriched cultures, Al was added to the polycarbonate culture vessels directly after filtration.

Cultures were grown at a temperature of 12°C and under a 14/10 h light/dark cycle and a light intensity of 300 to 400 μ Einstein/m²/s. The cultures were mixed by gentle rotation (1 rpm) on a roller bench. The initial cell density was ~50 cells/mL.

Before each experiment, all polycarbonate equipment was cleaned overnight with a hot detergent, rinsed several times with nanopure water, soaked overnight in 0.7% suprapure HNO₃, and rinsed again with nanopure water.

A detailed description of the experimental setup is presented by Van Beusekom and Weber (1992). Dissolved Al and Si levels of the culture medium are listed in Table 1 along with the order of magnitude of dissolved Al encountered in ocean waters.

2.2. Marine Diatom Samples

Two natural samples were used for of this study: (a) a benthic species assemblage from a Wadden Sea tidal flat (TF) and (b) a North Sea pelagic species *Biddulphia sinensis* (BS) (now referred to as *Odontella sinensis*). The benthic species assemblage was obtained by letting the diatoms migrate through three layers of lens tissue toward the light. The collecting technique relies on positive phototaxis and was first described by Eaton and Moss (1966). Triple layers of lens tissue are used on top of the sediment to ensure collection of sediment-free diatoms.

The pelagic sample was obtained by plankton tows. *B. sinensis* was collected in the Dogger Bank area of the North Sea.

The rationale behind this selection of samples is to provide a characterization of BSi before its incorporation to sediments. Samples were purified by repeated settling and decanting. Organic matter was removed by low temperature ashing.

2.3. Reference Mineral for XAS

Several reference compounds have been selected for XAS: albite and berlinite for tetrahedral Al and kaolinite for octahedral Al. In addition, muscovite, smectite, and illite have been selected as model compounds for minerals containing mixed 4- and 6-coordinated Al. The list is completed by a low-Al opal-A sample (Al/Si = 0.12), which is not of biogenic origin. A description of reference compounds is presented in Table 2.

3. ANALYTICAL METHODS

Al K-edge XANES and EXAFS spectra were collected on the SA 32 line (*E* range 0.8 to 3.5 keV) at the LURE/Super-ACO synchrotron radiation facility (Orsay, France). The storage ring was operating at 800 MeV positron energy and 100 to 300 mA positron current. The X-ray beam was monochromatized using a Yb66 double-crystal monochromator. Samples were powdered onto pure indium and mounted on a copper slide. Spectra were calibrated with a pure Al foil at the inflexion point of the K-edge (1559 eV) and recorded in fluorescence yield mode over a photon energy range of 1550 to 1600 eV (0.2-eV steps) for XANES and 1500 to 1820 eV (1-eV steps) for EXAFS. The intensity of the Al K-edge spectra was normalized relative to the atomic absorption above the threshold and linearly background fitted. The energy position of absorption edges of individual samples was determined from second derivative spectra. Background extracted EXAFS oscillations were Fourier transformed over the *k* range 1.5 to 7.5 Å^{-1} . The resulting Fourier transforms correspond to pseudoradial distribution functions around the Al atoms, which were not corrected for phase shift.

4. RESULTS

4.1. XANES Spectroscopy: Reference Compounds

Al K-edge XANES spectra of Al-bearing reference compounds are presented in Figure 1. Al K-edge XANES spectra of albite (tetrahedral Al), kaolinite (octahedral Al), and nonbiogenic opal-A (tetrahedral Al) are plotted in Figure 1a. Spectra of muscovite (mixed coordination), smectite (mixed coordination), and illite (mixed coordination) are shown in Figure 1b. The energy positions of main Al K-edge structures are summarized in Table 3.

Al K-edge XANES spectra of tetrahedral Al-bearing miner-

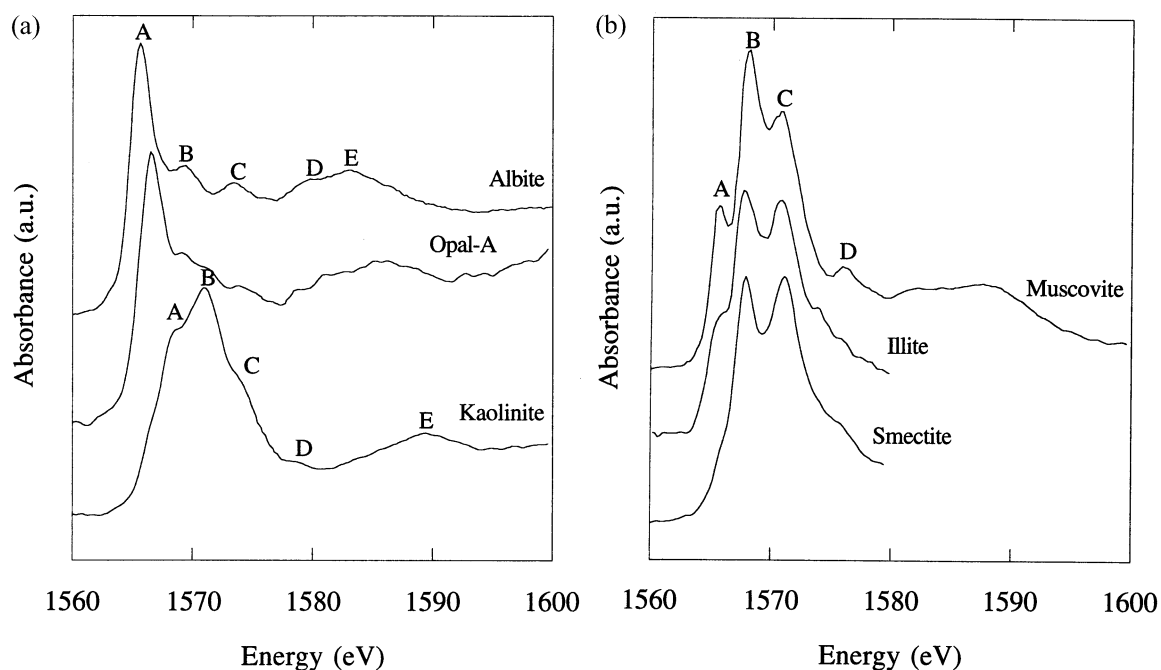


Fig. 1. Al K-edge X-ray absorption near-edge structure (XANES) spectra of reference compounds. (a) Crystalline model compounds albite (tetrahedral Al) and kaolinite (octahedral Al) compared to amorphous nonbiogenic opal-A (tetrahedral Al). (b) Model compounds for mixed 4- and 6-coordinated Al: muscovite, illite, and smectite. Positions in energy of main Al K-edge structures are exemplified on the XANES spectra for albite, kaolinite, and muscovite. Absorbance in arbitrary units (a. u.).

als, such as albite, are characterized by a strong and narrow single-edge maximum at 1565.4 eV. The edge maximum is shifted toward higher energy in the XANES spectra of minerals, which contain octahedral Al, with a strong influence from the geometry of the Al octahedron. The main absorption edge consists of several features located near 1570 eV, the relative intensity of which varies among the minerals investigated. In some phases, such as diaspore or pyrophyllite (Ildefonse et al., 1998), the edge maximum corresponds to the position of the low-energy resonance. By contrast, in kaolinite (Fig. 1a), the higher energy resonance is the most intense. In smectite and illite, both resonances have similar intensities (Fig. 1b). The Al K-edge XANES spectrum of muscovite (Fig. 1b) shows three edge maxima, one located at the energy position of tetrahedral Al and the two other corresponding to the two structures characteristic of octahedral Al. Above the absorption edge, all spectra show the presence of weak features, the positions and relative intensities of which are different among the various phases. XANES spectra are thus a sensitive tool not only for determining the coordination of Al in mineral compounds but also for revealing information on the medium-range structure

and the kind of phase in which Al occurs (Ildefonse et al., 1998).

4.2. XANES Spectroscopy: Diatom Samples

The Al K-edge XANES spectra of cultured diatom samples 87 and 103 indicate an identical position of the absorption edge and edge maximum. The weak structures present at higher energy do not occur at the same position in both samples (Fig. 2a). The features of sample 103 are located at an energy position similar to that observed in the crystalline reference albite (Fig. 1a), suggesting a fourfold coordination of Al. The spectra of diatom samples are less resolved than the crystalline reference, an indication of a strong structural disorder. In line with this observation, the spectra recorded for cultured diatoms closely correspond to that of nonbiogenic opal-A (Fig. 2a).

The spectra of the natural diatoms are identical for both samples (Fig. 2b). They show a more complex edge maximum than the spectra of cultured diatoms (Fig. 2a). The energy position of the absorption edge corresponds to that of albite, and the three resonances that constitute the main edge occur at

Table 3. Energy positions of main Al K-edge structures on X-ray absorption near-edge structure spectra of crystalline reference compounds.

Sample	A	B	C	D	E	Reference
Albite	1564.4	1569.5	1573.5	1579	1583	Kroll and Ribbe (1983)
Kaolinite	1568.2	1570.8				Bish and Von Dreele (1989)
Muscovite	1565.4	1567.8	1571.0			Rothbauer (1971)

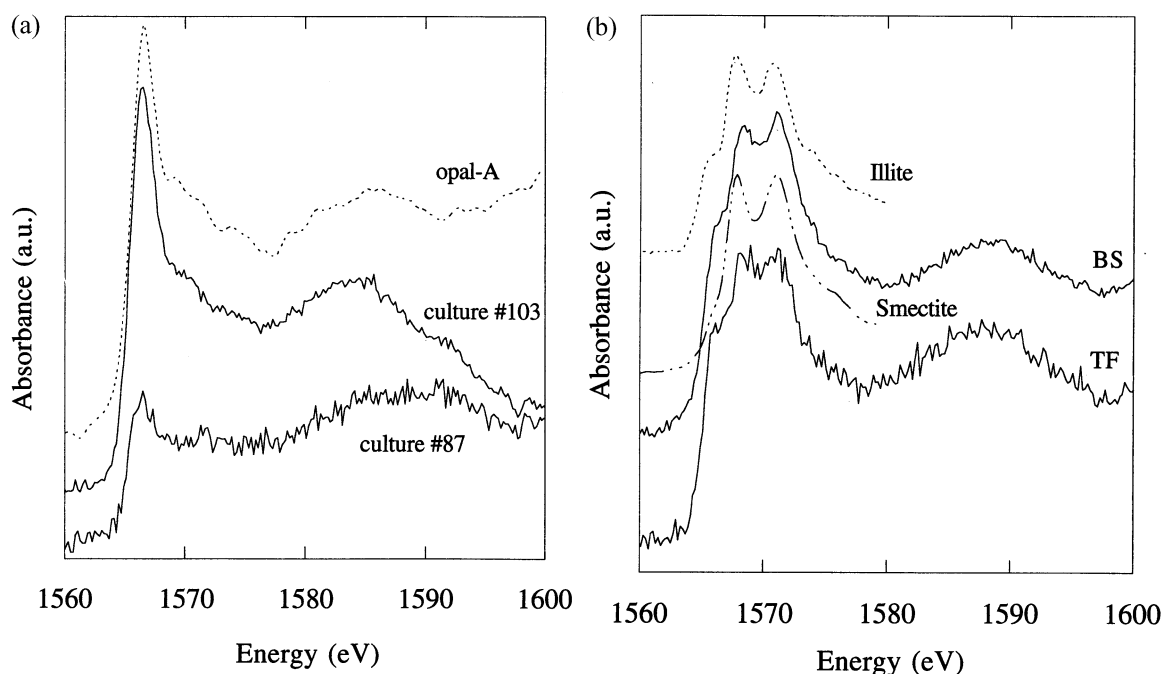


Fig. 2. (a) Al K-edge X-ray absorption near-edge structure (XANES) spectra of cultured diatom samples 103 and 87. The spectra of diatom samples yield an absorption edge and a maximum amplitude at the same energy position. The Al K-edge XANES spectra of cultured diatoms are compared to the spectrum of low-Al opal. The XANES multiple-scattering features are consistent with a disorder surrounding clusters and imply corner sharing tetrahedra. (b) Al K-edge XANES spectra of marine diatom samples TF and BS. Spectra of smectite and illite are included for comparison. Both diatom samples process spectra close to identical. While the first resonance is characteristic of fourfold-coordinated Al, the two other resonances correspond to sixfold-coordinated Al. The shapes of the adsorption edges of diatom samples and smectite are similar. The relative intensities of XANES structures indicates the coexistence of structural Al with a smectite- or illite-type clay component. Absorbance in arbitrary units (a.u.).

the same position as in smectite and illite. The first resonance is characteristic of fourfold-coordinated Al, and the two further resonances correspond to sixfold-coordinated Al, by comparison with the spectra of crystalline references. A high-energy feature is observed near 1590 eV. This position in energy is similar to that observed in spectra of octahedral Al (feature E, kaolinite, Fig. 1a). Al thus appears to be present with mixed coordination numbers in both natural samples.

4.2. EXAFS Spectroscopy: Cultured Diatom Samples

Al K-edge EXAFS spectra were recorded for cultured diatom samples 87 and 103. Background subtracted Al K-edge EXAFS spectra of diatom cultures 87 are presented in Figure 3a as a function of wave vector k compared to berlinite. Berlinite is selected as a reference compound for this comparison because of its regular and well-described structure. Because of the proximity of the Si-K absorption edge, only a limited energy range is accessible, and the information is mostly limited to the nearest neighbors, as shown by the presence of one major contribution on the Fourier transform (Fig. 3b). The close match of the module and the imaginary part of the Fourier transforms indicates identical coordination number and Al-O distances in sample 87 and berlinite. The energy positions of absorption edges and the mean Al-O distances of sample compounds 87 and 103, which were obtained by fitting

the signal corresponding to the first shell of neighbors, are summarized in Table 4.

5. DISCUSSION

5.1. Structural Interpretation of Spectra of Cultured Diatoms

Aluminum may enter the framework of amorphous silica by two distinct structural processes (Narshneyer, 1994). It may enter as a network former, preserving the three-dimensional structure built by the corner sharing SiO_4 tetrahedra, provided there is charge compensation by alkalis or alkaline earths located in a nearby position. Alternatively, a nonbridging oxygen is created by the presence of two octahedral Al atoms linked to an oxygen belonging to a SiO_4 tetrahedron. At low temperature, Al is encountered in poorly ordered aluminosilicate phases formed during continental weathering, such as allophanes, imogolites, and Al-bearing amorphous silica (opal-A). The presence of both 4- and 6-coordinated Al in natural allophanes has been recognized by various authors. In nonbiogenic low-Al opal-A, all Al occurs in fourfold coordination and plays the structural role of a network former in the three-dimensional structure (Ildefonse and Calas, 1997).

The XANES and EXAFS data shown in this study are similar for cultured diatoms and crystalline minerals in which Al is tetrahedrally coordinated like albite (Fig. 1a) or berlinite

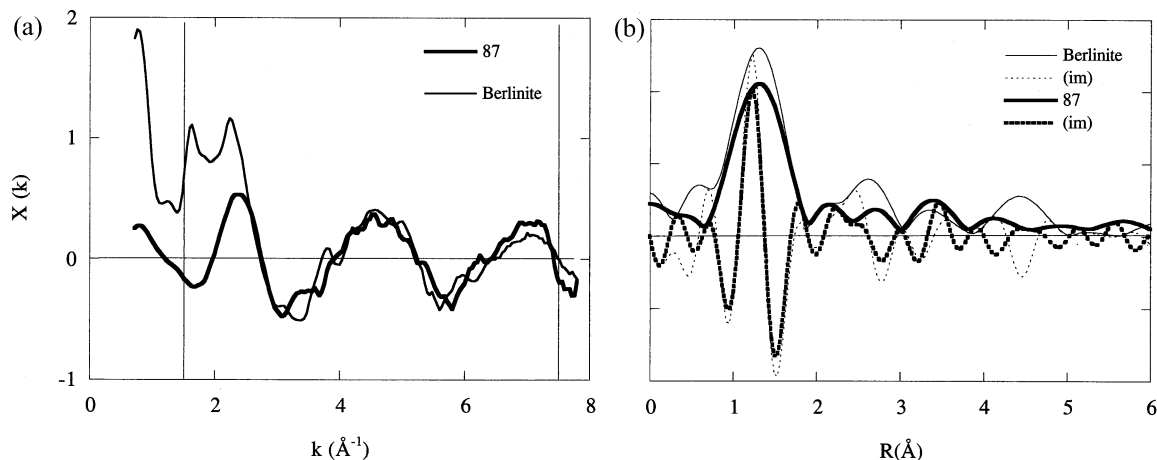


Fig. 3. Al K-edge extended X-ray absorption fine structure (EXAFS) spectra of cultured diatom sample 87 compared to model compound berlinite. (a) Background-subtracted EXAFS plotted as a function of wave vector k . Extracted EXAFS spectra were Fourier transformed over the k range of 1.5 to 7.5 \AA^{-1} (vertical bars). (b) Module (FT) and imaginary part (im FT) of Fourier transforms corresponding to the Al K-edge EXAFS spectra. Distances are not corrected for phase shift.

(Fig. 3). The energy position of the absorption edge and the mean Al-O distance are comparable. This indicates that Al is predominantly fourfold coordinated in samples of diatom cultures. XANES spectroscopy is sensitive to the medium-range organization around the absorbing atom. XANES spectra may thus be used to understand the structural significance of the tetrahedral coordination of Al within the silica framework of cultured diatom samples. Full multiple-scattering calculations have been made for the Al K-edge XANES spectra of the reference minerals used in this study (Cabaret et al., 1996). The main resonance corresponds to atomic-like levels and gives direct information on the coordination state of Al. By contrast, the higher energy resonances correspond to multiple scattering and are related to the geometrical arrangement of the nearest and next nearest neighbors around Al. The first coordination shell gives rise to a single, broad resonance close to 1585 eV , characteristic of a tetrahedral coordination. Further resonances are found when considering the contribution from second and further shells at the same time as the broad resonance shifts toward lower energy. The low intensity of these features indicates a strong disorder around Al, which is characteristic of the insertion of Al in the amorphous structure of biogenic opal. Along this line of thought, the differences between samples 87 and 103 may be explained by a stronger disorder in the former. The presence of resonances at 1571 and 1574 eV on the XANES spectrum of sample 103 indicates multiple-scattering events in clusters based on corner-sharing silicate and aluminate tetrahedra. These clusters have diameters between 9 and 11.7 \AA .

Table 4. Energy positions of absorption edges (a-edge) and mean Al-O distances of diatom samples. Al^{IV}-O refers to fourfold coordination.

Sample ID	a-edge (eV)	Al ^{IV} -O (\AA)
Berlinite	1565.8 ± 0.2	1.74
Diatom culture 87	1565.2	1.73 ± 0.02
Diatom culture 103	1565.2	1.78

The location of Al in cultured diatoms could be explained by three hypotheses. First, Al could be present within trace aluminosilicates. Framework silicates are the only low-temperature minerals in which Al is exclusively in tetrahedral coordination. The corresponding spectra are characterized by the occurrence of well-defined characteristic multiple-scattering features above the main edge, as exemplified for albite in Figure 1a. These features are better resolved in albite and other crystalline references (Ildefonse et al., 1998) than on the cultured diatom spectra. The presence of trace crystalline aluminosilicates can thus be ruled out. Aluminum could also be present in trace aluminosilica gels included inside the diatom frustules. To yield the measured bulk Al levels, these included gels must be concentrated in Al. However, in natural, nonbiogenic aluminosilica gels and poorly ordered phases such as allophanes and imogolites (Ildefonse et al., 1994), Al occupies both coordination states (6 and 4). This is not consistent with the XANES and EXAFS results presented for cultured diatoms. The only occurrence of exclusively tetrahedral Al is in nonbiogenic opals that have low Al contents ($<1\%$). The chemical analysis of the bulk material agrees with the Al content of low-Al opals. The XANES multiple-scattering features are consistent with a disorder surrounding clusters and imply corner-sharing tetrahedra, as expected in a low-Al opal. In addition, the considerations on multiple-scattering events at the origin of the major XANES resonances indicate a medium-range order, implying an Al-bearing tetrahedron connected to four silicate tetrahedra, with some longer range ordering. We conclude that the XANES and EXAFS data of cultured diatoms indicate that Al belongs to the silica framework synthesized by the organism.

The presence of trace elements such as alkalis or alkaline earths may reflect processes of charge compensation at the origin of the stability of tetrahedral Al in this peculiar surrounding. Substitution of Si^{4+} by Al^{3+} creates a negative charge which needs to be balanced by alkali or alkaline earth cations. In cultured samples, Ca correlates with Al in such a way that it may balance the charge deficit around Al tetrahedra. The Ca-

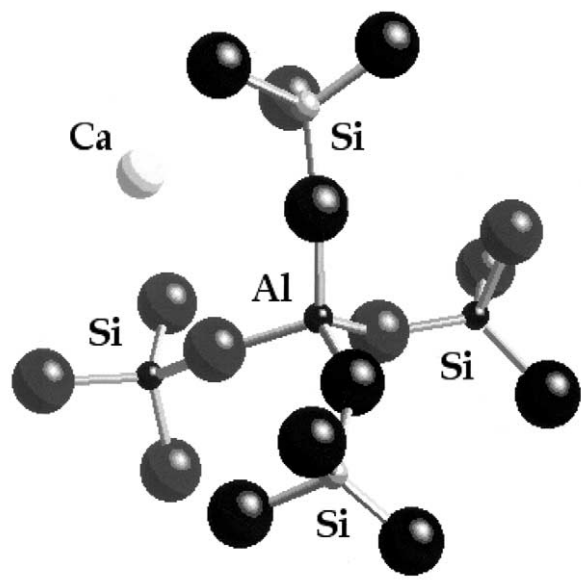


Fig. 4. A structural model of biogenic silica. Al enters the structure as a network former preserving the three-dimensional environment built by the corner-sharing SiO_4 tetrahedra. Substitution of Si^{4+} by Al^{3+} creates a unit negative charge. The compositional analyses of diatom samples suggest a charge compensation by Ca^{2+} .

to-Al atomic abundance relationship (Table 1) is given as $\text{Ca} = 0.55 \times \text{Al} + 0.0015$ (Beck et al., in press). The slope of the Ca-to-Al relationship is close to 0.5, which indicates that Ca alone may be responsible for the charge compensation of the substituted Al in BSi synthesized by cultured diatoms. The resulting structural model of BSi is presented in Figure 4.

The interlinkage of Al and Si tetrahedra within diatom frustules is a strong indication of the incorporation of Al during the biosynthesis of frustule silica and does not result from subsequent contamination. It also provides a structural explanation for the effect of Al on the solubility of BSi. The structural position of Al is unusual at low temperature, at which Al is generally found in octahedral coordination. This structural peculiarity is only observed at low Al concentrations, provided there is charge compensation by neighbor cations. It reflects the structural constraints imposed by the Si framework.

5.2. Structural Interpretation of Spectra of Natural Diatoms

In experimental spectra of natural diatoms, the well-identified absorption edges of tetrahedral and octahedral Al indicate the presence of the two coordination numbers. The mixed coordination might be due to the presence of Al exclusively in clay minerals such as illite or smectite, in which Al has the two coordination numbers, without a contribution of Al associated to the diatoms. As indicated above, the strong intensity of the tetrahedral component as well as the relative intensity of the two edge crest features indicates that the first explanation is not consistent with the observed XANES structures.

An alternative explanation may be the coexistence of the structural Al in BSi with a clay component, which will significantly increase the relative intensity of the feature related to

the presence of tetrahedral Al. The relative intensity of the tetrahedral component is not compatible with the presence of a muscovite clay fraction, which might indicate a higher contribution from octahedral Al. The relative intensity of the two edge components is also different between natural diatoms and muscovite, with an inversion of the relative intensities of these features. The shape of the main edge is thus not in favor of the presence of muscovite or of aluminosilicate gels, in which the low-energy resonance related to octahedral Al is the most intense. The higher intensity of the high-energy resonance in diatom samples might originate from the presence of smectite- or illite-type clay phases, which process a similar edge shape (Fig. 2b). The presence of other phases, such as gibbsite, may be excluded despite a similar relative intensity of the two main edge resonances. The high-energy feature characteristic of these phases is much broader and less resolved than on the spectra of natural diatoms (Ildefonse et al., 1998). Spectra of natural diatoms are thus consistent with the coexistence of structural Al in fourfold coordination within BSi and Al bound within a smectite- or illite-type phase. Smectite and illite are major components of the clay fraction of North Sea sediments (Zöllmer and Irion, 1993). Despite our best efforts to isolate clean diatom frustules, a contamination by adhering clay particles cannot be excluded at this stage. We conclude that by analogy to the cultures, the fourfold coordination reflects Al incorporated during frustule biosynthesis, while the smectite- or illite-type phase probably corresponds to adhering clay particles.

5.3. The Coupling of Al and Si Geochemical Cycles

Al-K XANES and EXAFS spectra collected for diatoms demonstrate for the first time the structural association between Al and Si in BSi and lend support to the close coupling of Al and Si marine geochemical cycles by diatom dynamics. The coupling of marine geochemical cycles of Al and Si through the interaction between dissolved Al and biogenic siliceous particles was proposed over 20 yr ago. Active biological uptake of Al by diatoms during biosynthesis and its incorporation into the siliceous frustule was inferred from the apparent Al-Si covariation of pelagic dissolved Si and Al levels (Van Bennekom and Van Der Gaast, 1976; Mackenzie et al., 1978; Stoffyn and Mackenzie, 1982; Chou and Wollast, 1997). This covariation, which implies a nutrient-like distribution for dissolved Al in ocean waters, is however restricted to particular oceanic environments such as estuaries or the Mediterranean Sea. In the open ocean, the vertical distribution of dissolved Al and its distinct differences between ocean basins suggest a control of dissolved Al dominated by scavenging (Li, 1991). The strong affinity of biogenic siliceous particles for dissolved Al is corroborated by the observation that reduced levels of dissolved Al are associated with high diatom production (Orlans and Bruland, 1986; Van Beusekom, 1988). The exact nature of the association between dissolved Al and biogenic siliceous particles, however, remains controversial.

Previous experiments with diatom cultures supported Al removal from seawater by biologic uptake (Stoffyn, 1979; Van Bennekom et al., 1991; Van Beusekom and Weber, 1992, 1995). Other studies stressed the importance of a primarily inorganic removal mechanism of Al by its association with

particle surfaces in controlling the distribution of dissolved Al (Hydes, 1979; Orians and Bruland, 1985; Moran and Moore, 1988, 1992). In living diatoms, frustules are protected from alteration by the organic matrix in which the BSi building blocks are encased. The protective role of this organic matrix was highlighted by Bidle and Azam (1999). The authors demonstrated the role of bacteria in controlling the dissolution rate of BSi. The underlying mechanism involves the removal of the organic matrix by bacterial activity followed by the exposure of frustule walls to undersaturated seawater. As long as the organism is alive, the siliceous skeleton is shielded from the outer environment. The presence of Al in frustules of living cultured diatoms in exclusively fourfold coordination thus strongly suggests its incorporation during biosynthesis.

Because of the strong inhibition of BSi solubility by minor amounts of Al, its incorporation at the stage of biosynthesis is expected to result in varying solubilities of the BSi flux deposited at the sediment-water interface. This line of thought is compatible with regional variations in the solubility of BSi inferred from pore water data (Archer et al., 1993; McManus et al., 1995). It suggests a possible contribution of surface ocean processes to the control of BSi solubility through the coupling of biogeochemical Al and Si cycles. Aluminum is added to open ocean waters by the deposition of eolian dust of continental origin followed by the partial dissolution of the aluminosilicate fraction (Measures and Brown, 1996; Measures and Vink, 2000). Without denying the importance of postdepositional uptake of Al by diatom frustules during early diagenesis (Van Bennekom et al., 1989, 1991; Dixit et al., 2001), the regional variability of BSi solubility should in part reflect dissolved Al availability and thus be related to its main source: the partial dissolution of the aluminosilicate fraction of continental dust.

6. CONCLUSIONS

Al K-edge XANES and EXAFS spectra collected for diatoms underline the structural association between Al and Si in diatom frustules. In samples of cultured diatoms, Al is present exclusively in fourfold coordination. The location and relative intensities of XANES features suggest the structural insertion of tetrahedral Al inside the silica framework synthesized by the organism. The peculiar structural position of Al within the BSi framework is invoked to explain the inhibiting effect of Al on the solubility of BSi (decrease of solubility). The incorporation of Al at the stage of biosynthesis is expected to result in varying solubilities of the flux of BSi deposited at the sediment-water interface.

In natural diatom samples, Al is present in mixed six- and fourfold coordination. The relative intensities of XANES structures indicate the coexistence of structural Al with a smectite or illite component. While greatest care was taken to avoid contamination of samples collected in the marine environment by adhering mineral particles, it cannot be excluded that the clay component corresponds to trace mineral particles occluded in frustule pores.

Acknowledgments—The first author dedicates this study to Prof. R. Wollast (Laboratoire d'Océanographie Chimique, Université Libre de Bruxelles) for initiating her to the silica problem during her Ph.D. work. She thanks F. T. Mackenzie for many fruitful discussions during

the past years. This manuscript benefited from constructive comments by P. Anschutz, P. Van Cappellen, and P. N. Froelich. This study was carried out at the Laboratoire d'Utilisation du Rayonnement Electromagnétique (LURE), Orsay, France (LURE project ID CS012-98). This is LSCE contribution 0651.

Associate editor: R. H. Byrne

REFERENCES

- Archer D., Lyle M., Rodgers K., and Froelich P. (1993) What controls opal preservation in tropical deep-sea sediments? *Paleoceanogr.* **8**, 7–21.
- Barker P., Fontes J.-C., Gasse F., and Druart J.-C. (1994) Experimental dissolution of diatom silica in concentrated salt solutions and implications for paleoenvironmental reconstructions. *Limnol. Oceanogr.* **39**, 99–110.
- Beck L., Gehlen M., Flank A.-M., Van Bennekom J. A., and Van Beusekom J. E. E. (in press) The structural characterization of biogenic opal: An example of the complementarity of PIXE and XAS applied to environmental sciences. *Nucl. Instr. Meth.*
- Bidle K. D. and Azam F. (1999) Accelerated dissolution of diatom silica by marine bacterial assemblages. *Nature* **397**, 508–512.
- Bish D. L. and Von Dreele R. B. (1989) Rietveld refinement of non-hydrogen atomic positions in kaolinite. *Clays Clay Miner.* **37**, 289–296.
- Brown G. E., Jr., Calas G., Waychunas G. A., and Petiau J. (1988) X-ray absorption spectroscopy and its applications in mineralogy and geochemistry. In *Reviews in Mineralogy: Spectroscopic Methods in Mineralogy and Geology* (ed. F. C. Hawthorne), pp. 431–512. Mineralogical Society of America, Washington, DC.
- Cabaret D., Sainctavit P., Ildefonse P., and Flank A.-M. (1996) Full multiple scattering calculations on silicates and oxides at the Al K edge. *J. Phys.: Condens. Matter* **8**, 3691–3704.
- Calas G., Bassett W. A., Petiau J., Steinberg M., Tchoubar D., and Zarka A. (1984) Some mineralogical applications of synchrotron radiation. *Phys. Chem. Miner.* **11**, 17–36.
- Chou L. and Wollast R. (1997) Biogeochemical behavior and mass balance of dissolved aluminum in the western Mediterranean Sea. *Deep-Sea Res.* **44**, 741–768.
- Dixit S., Van Cappellen P., and Van Bennekom A. J. (2001) Processes controlling solubility of biogenic silica and pore water build-up of silicic acid in marine sediments. *Mar. Chem.* **73**, 333–352.
- Eaton J. W. and Moss B. (1966) The estimation of numbers and pigment content in epipelagic algal populations. *Limnol. Oceanogr.* **11**, 584–595.
- Fanning K. A. and Pilon M. E. Q. (1974) The diffusion of dissolved silica out of deep-sea sediments. *J. Geophys. Res.* **79**, 1293–1297.
- Garrels R. M. and Mackenzie F. T. (1971) *The Evolution of Sedimentary Rocks*. Norton, New York.
- Guillard R. R. L. and Ryther J. H. (1962) Studies of marine planktonic diatoms. I. *Cyclotella nana* Hustedt and *Detonula confervacea* (Cleve) Gran. *Can. J. Microbiol.* **8**, 229–239.
- Hurd D. C. (1973) Interactions of biogenic opal, sediment and seawater in the central equatorial Pacific. *Geochim. Cosmochim. Acta* **37**, 2257–2281.
- Hurd D. C. and Birdwhistell S. (1983) On producing a more general model for biogenic silica dissolution. *Am. J. Sci.* **283**, 1–28.
- Hurd D. C., Pankratz H. S., Aspen V., Fugate J., and Morrow H. (1981) Changes in the physical and chemical properties of biogenic silica from the central equatorial Pacific. Part III. Specific pore volume, mean pore size, and skeletal ultrastructure of acid cleaned samples. *Am. J. Sci.* **281**, 833–895.
- Hydes D. J. (1979) Aluminum in seawater: Control by inorganic processes. *Science* **205**, 1260–1262.
- Ildefonse P. and Calas G. (1997) Natural gels: Crystal-chemistry of short range ordered components in Al, Fe and Si systems. In *Actes des journées sur le verre*, Université d'été CEA/Valrhô, 31 Août–7 Septembre 1997, Méjannes-Le-Clap, pp. 461–468.
- Ildefonse P., Kirkpatrick R. J., Montez B., Calas G., Flank A.-M., and Lagarde P. (1994) 27-Al NMR and aluminum X-ray absorption near edge structure study of imogolite and allophanes. *Clays Clay Miner.* **42**, 276–287.

- Ildefonse P., Cabaret D., Sainctavit P., Calas G., Flank A.-M., and Lagarde P. (1998) Aluminum X-ray absorption near edge structure in model compounds and earth's surface minerals. *Phys. Chem. Min.* **25**, 112–121.
- Iler R. K. (1973) Effect of adsorbed alumina on the solubility of amorphous silica in water. *J. Colloid Interface Sci.* **43**, 399–408.
- Jumas J. C., Goiffon A., Capelle B., Zarka A., Doukhan J. C., Schwartzel J., Détaint J., and Philippot E. (1987) Crystal growth of berlinite, AlPO_4 : Physical characterization and comparison with quartz. *J. Cryst. Growth* **80**, 133–148.
- Kamatani A., Riley J. P., and Skirrow G. (1980) The dissolution of opaline silica of diatom tests in sea water. *J. Oceanogr. Soc. Jap.* **36**, 201–208.
- Kroll H. and Ribbe P. H. (1983) Lattice parameters, composition and Al, Si order in alkali feldspars. *Rev. Miner.* **2**, 57–99.
- Lawson D. S., Hurd D. C., and Pankratz H. S. (1978) Silica dissolution rates of decomposing phytoplankton assemblages at various temperature. *Am. J. Sci.* **278**, 1373–1393.
- Leinen M., Cwienk D., Heath G. R., Bisacaye P. E., Kolla, V., Thiede J., and Dauphin J. P. (1986) Distribution of biogenic silica and quartz in recent deep-sea sediment. *Geology* **14**, 199–203.
- Lewin J. C. (1961) The dissolution of silica from diatom walls. *Geochim. Cosmochim. Acta* **21**, 182–198.
- Lyle M., Murray D. W., Finney B. P., Dymond J., Robbins J. M., and Brooksforce K. (1988) The record of late Pleistocene biogenic sedimentation in the eastern tropical Pacific Ocean. *Paleoceanogr.* **3**, 39–59.
- Mackenzie F. T. and Garrels R. M. (1966) Chemical mass balance between rivers and oceans. *Am. J. Science.* **264**, 507–525.
- Mackenzie F. T., Stoffyn M., and Wollast R. (1978) Aluminum in seawater: Control by biological activity. *Science* **199**, 680–682.
- Mackenzie F. T., Ristvet B. L., Thorstenson D. C., Lerman A., and Leeper R. H. (1981) Reverse weathering and chemical mass balance in a coastal environment. In *River Inputs to the Ocean* (eds. J.-M. Martin, J. D. Burton, and D. Eisma), pp. 152–187. United Nations Environment Programme, United Nations Educational, Scientific, and Cultural Organization, Geneva, Switzerland.
- Martin J. H. and Knauer G. A. (1973) The elemental composition of plankton. *Geochim. Cosmochim. Acta* **37**, 1639–1653.
- McManus J., Hammond D. E., Berelson W. M., Kilgore T. E., De Master D. J., Ragueneau O. G., and Collier R. W. (1995) Early diagenesis of biogenic opal: Dissolution rates, kinetics, and paleoceanographic implications. *Deep-Sea Res.* **42**, 871–903.
- Measures C. I. and Brown E. T. (1996) Estimating dust input to the Atlantic Ocean using surface water Al concentrations. In *The Impact of Desert Dust Across the Mediterranean* (eds. J. Guerzoni and R. Chester), pp. 301–311. Kluwer, Dordrecht, the Netherlands.
- Measures C. I. and Vink S. (2000) On the use of dissolved aluminum in surface waters to estimate dust deposition to the ocean. *Global Biogeochem. Cycles* **14**, 317–327.
- Michalopoulos P. and Aller R. C. (1995) Rapid clay mineral formation in Amazon delta sediments: Reverse weathering and oceanic elemental cycles. *Science* **270**, 614–617.
- Michalopoulos P., Aller R. C., and Reeder R. J. (2000) Conversion of diatoms to clays during early diagenesis in tropical, continental shelf muds. *Geology* **28**, 1095–1098.
- Moran S. B. and Moore R. M. (1988) Evidence from mesocosm studies for biological removal of dissolved aluminium from sea water. *Nature* **335**, 706–708.
- Moran S. B. and Moore R. M. (1992) Kinetics of the removal of dissolved aluminium by diatoms in seawater: A comparison with thorium. *Geochim. Cosmochim. Acta* **56**, 3365–3374.
- Morel F. M. M., Ruether J. G., Jr., Anderson D. M., and Guillard R. R. M. (1979) Aquil: A chemically defined phytoplankton culture medium for trace metal studies. *J. Phycol.* **15**, 134–141.
- Narshneyer A. K. (1994) *Fundamentals of Inorganic Glasses*. Academic Press, San Diego, CA.
- Nelson D. M., Tréguer P., Brzezinski M. A., Leynaert A., and Quéguiner B. (1995) Production and dissolution of biogenic silica in the ocean: Revised global estimates, comparison with regional data and relationship to biogenic sedimentation. *Global Biogeochem. Cycles* **9**, 359–372.
- Orians K. J. and Bruland K. W. (1985) Dissolved aluminium in the central North Pacific. *Science* **316**, 427–429.
- Orians K. J. and Bruland K. W. (1986) The biogeochemistry of aluminum in the Pacific Ocean. *Earth Planet. Sci. Lett.* **78**, 397–410.
- Rabouille C., Gaillard J. F., Tréguer P., and Vincendeau M. A. (1997) Biogenic silica recycling in surficial sediments across the polar front of the Southern Ocean (Indian Sector). *Deep-Sea Res.* **44**, 1151–1176.
- Rea D. K., Piasis N. G., and Newberry T. L. (1991) Late Pleistocene paleoclimatology of the central equatorial Pacific: Flux patterns of biogenic sediments. *Paleoceanogr.* **6**, 6227–6244.
- Ristvet B. L. (1978) *Reverse Weathering Reactions Within Recent Nearshore Marine Sediments, Kaneohe Bay, Oahu*. Ph.D. thesis, Test Directorate Field Command, Kirtland Air Force Base, Albuquerque, NM.
- Rothbauer V. R. (1971) Untersuchungen eines 2M_1 -Muskovits mit Neutronenstrahlen. *N. Jahrb. Mineral. Mh.* 143–154.
- Sayles F. L., Deuser W. G., Goudreau J. E., Dickinson W. H., Jickells T. D., and King P. (1996) The benthic cycle of biogenic opal at the Bermuda Atlantic Time Series site. *Deep-Sea Res.* **43**, 383–409.
- Schink D. R., Fanning K. A., and Pilson M. E. Q. (1974) Dissolved silica in the upper pore waters of the Atlantic Ocean floor. *J. Geophys. Res.* **79**, 2243–2250.
- Stoffyn M. (1979) Biological control of dissolved aluminum in seawater: Experimental evidence. *Science* **203**, 651–653.
- Stoffyn M. and Mackenzie F. T. (1982) Fate of dissolved aluminum in the oceans. *Mar. Chem.* **11**, 105–127.
- Stone W. E. E., Shafei G. M. S., Sanj J., and Selim A. (1993) Association of soluble aluminum ionic species with a silica-gel surface. A solid-state NMR study. *J. Phys. Chem.* **97**, 10127–10132.
- Tréguer P., Nelson D. M., Van Bennekom A. J., De Master D. J., Leynaert A., and Quéguiner B. (1995) The silica balance in the world ocean—A reestimate. *Science* **268**, 375–379.
- Van Bennekom A. J. and Van Der Gaast S. J. (1976) Possible clay structures in the frustules of living diatoms. *Geochim. Cosmochim. Acta.* **40**, 1149–1152.
- Van Bennekom A. J., Jansen F., Van Der Gaast S., Van Iperen J., and Pieters J. (1989) Aluminum-rich opal: An intermediate in the preservation of biogenic silica in the Zaire (Congo) deep-sea fan. *Deep-Sea Res.* **36**, 173–190.
- Van Bennekom A. J., Buma A. G. J., and Nolting R. F. (1991) Dissolved aluminum in the Weddell-Scotia confluence and effect of Al on the dissolution kinetics of biogenic silica. *Mar. Chem.* **35**, 423–434.
- Van Beusekom J. E. E. (1988) Distribution of dissolved aluminium in the North Sea: Influence of biological processes. In *Biogeochemistry and Distribution of Suspended Matter in the North Sea and Implications to Fisheries Biology* (eds. S. Kempe, G. Liebezeit, V. Dethlefsen, and U. Harms) Mitt. Geol.-Paläont. Inst., Univ. Hamburg, SCOPE/UNEP Sonderbd., **65**, 137–151.
- Van Beusekom J. E. E. (1991) Wechselwirkungen zwischen gelöstem Aluminium und Phytoplankton in marinen Gewässern. Thesis, University of Hamburg.
- Van Beusekom J. E. E. and Weber A. (1992) Decreasing diatom abundance in the North Sea: The possible significance of aluminium. In *Marine Eutrophication and Population Dynamics* (eds. G. Colombo et al.), pp. 121–127. Olsen and Olsen, Fredensborg, Denmark.
- Van Beusekom J. E. E. and Weber A. (1995) Der Einfluß von Aluminium auf das Wachstum und die Entwicklung von Kieselalgen in der Nordsee. *Germ. J. Hydrogr.* **5**, 213–220.
- Van Beusekom J. E. E., Van Bennekom A. J., Tréguer P., and Morvan J. (1997) Aluminium and silicic acid in water and sediments of the Enderby and Crozet Basins. *Deep-Sea Res. II* **44**, 987–1003.
- Van Cappellen P. (1996) Reactive surface area control of the dissolution kinetics of biogenic silica in deep-sea sediments. *Chem. Geol.* **132**, 125–130.
- Van Cappellen P. and Qiu L. (1997a) Biogenic silica dissolution in sediments of the Southern Ocean. I. Solubility. *Deep-Sea Res.* **44**, 1109–1128.
- Van Cappellen P. and Qiu L. (1997b) Biogenic silica dissolution in sediments of the Southern Ocean. II. Kinetics. *Deep-Sea Res.* **44**, 1129–1149.
- Zöllmer V. and Irion G. (1993) Clay mineral and heavy metal distributions in the northeastern North Sea. *Mar. Geol.* **111**, 223–230.